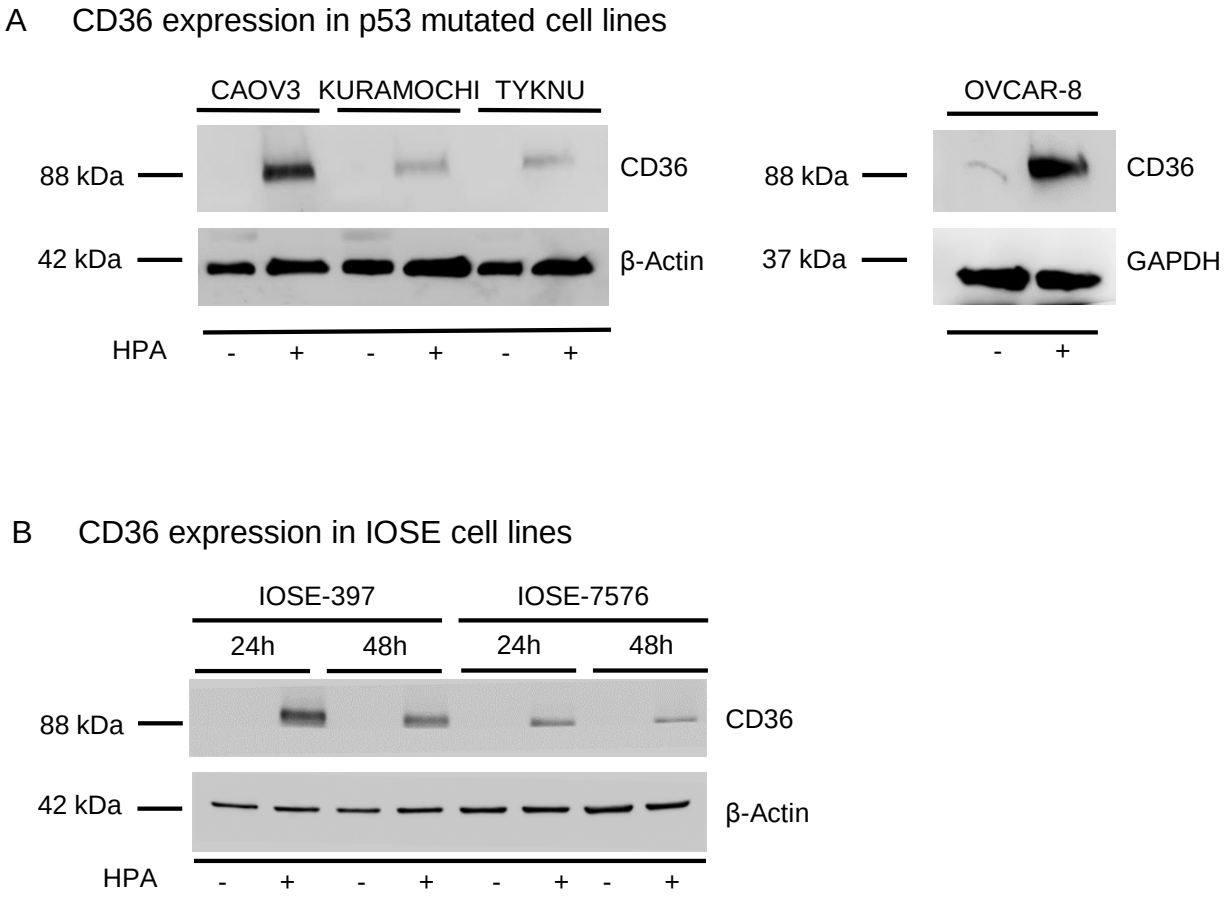

Supplementary Figure 1.
(a) CD36 protein expression in p53 mutated ovarian cancer cell lines incubated with (+) or without (-) human primary adipocytes (HPA) for 24 hrs
(b) CD36 protein expression in two immortalized, but non-tumorigenic, ovarian surface epithelial cell lines (IOSE) incubated with (+) or without (-) human primary adipocytes (HPA) at the indicated time points.

C Western blot time course of CD36 expression

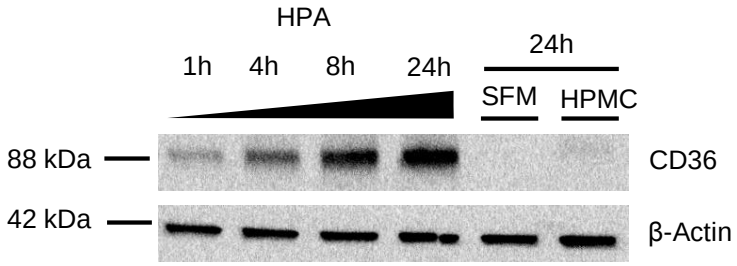

D CD36 mRNA expression

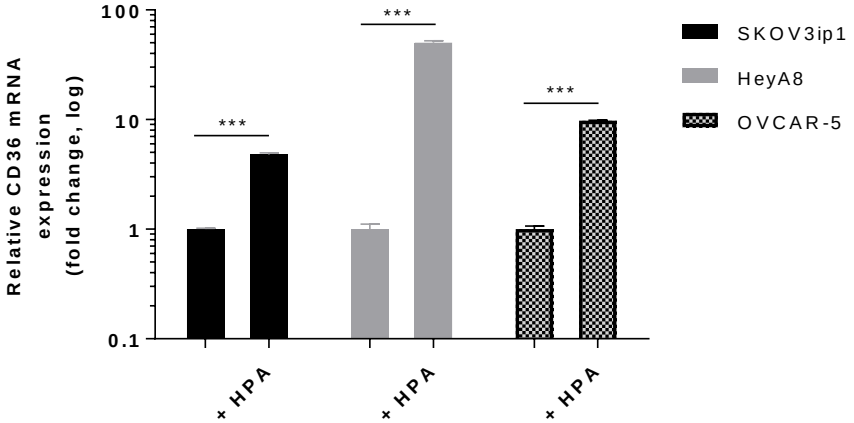

E Subcellular fractionation time course

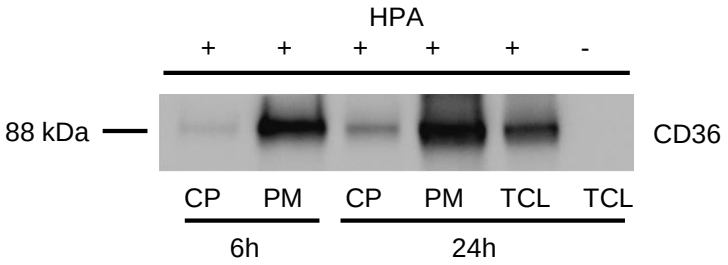

Supplementary Figure 1 continued.

(c) Time course of CD36 protein expression in SKOV3ip1 cells incubated with human primary adipocytes (HPA) or with serum free media (SFM) and human primary mesothelial cells (HPMC).

(d) Quantitative real-time PCR analysis of CD36 mRNA expression in ovarian cancer cell lines incubated in the absence and presence (+ HPA) of human primary adipocytes (HPA) for 24 h. Results are expressed as fold-change of CD36 *versus* basal level normalized to GADPH and displayed on a logarithmic scale. Bars represent mean ± s.e.m. Data are representative of two independent experiments performed in triplicates. ***p< 0.001

(e) Subcellular localization of CD36 protein over time. SKOV3ip1 cells were grown in the presence (+) or absence (-) of HPA. Cells were either lysed to obtain total cellular lysate (TCL) or fractionated into cytoplasmic (CP) and plasma membrane (PM) fractions.

A CD36 shRNA validation, mRNA and protein– SKOV3ip1

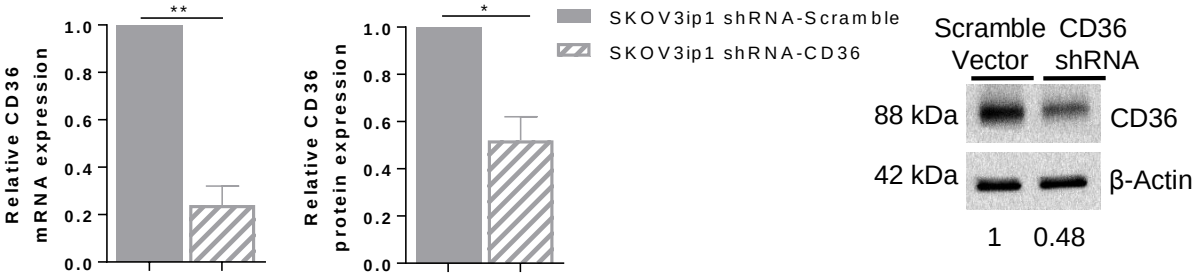

B Constitutive and Inducible CD36mRNA expression

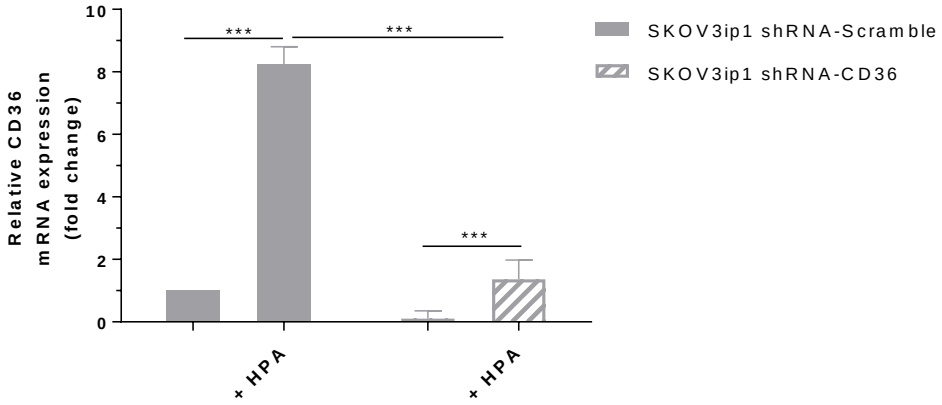

Supplementary Figure 2.
(a) Left Panel: Quantitative Real-Time (qRT)-PCR analysis of CD36 mRNA and immunoblotting for CD36 protein in cells stably transfected with non-targeting control, scramble vector (SKOV3ip1 shRNA-Scramble) or a vector targeting CD36 (SKOV3ip1 shRNA-CD36). Right panel: Representative immunoblot with densitometric analysis showing fold change in protein levels compared with cells transfected with control shRNA. qRT-PCR and immunoblotting were repeated three times with similar results. Bars represent mean ± s.e.m., **p< 0.01, *p< 0.05.
(b) qRT-PCR analysis of constitutive and inducible CD36mRNA levels in the scramble control (SKOV3IP1 shRNA-Scramble) and CD36 shRNA-1 transduced (SKOV3ip1 shRNA-CD36) cells. Bars represent mean ± s.e.m., ***p< 0.001. (n=3)

C Proliferation assay

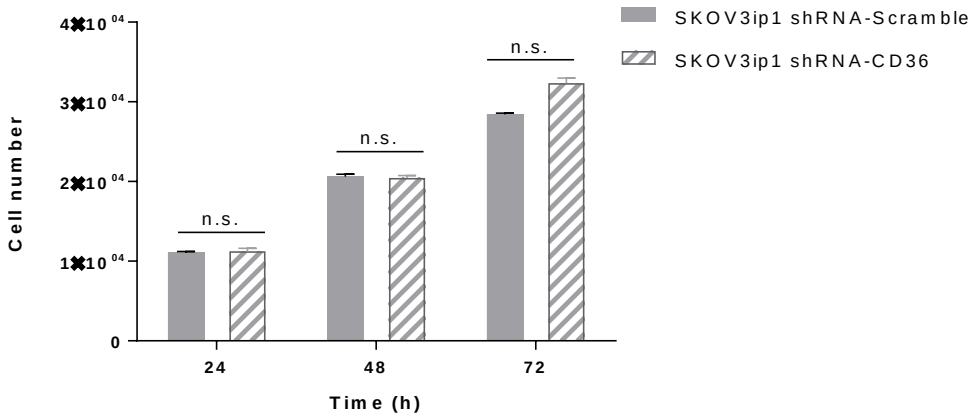

D Viability assay

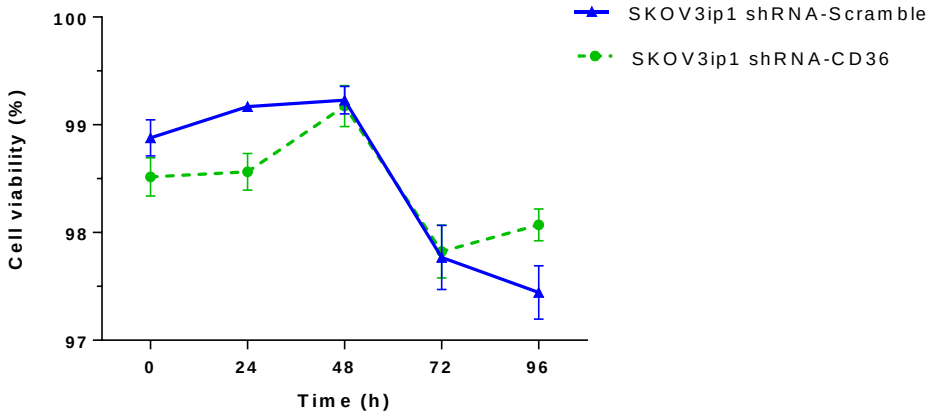

Supplementary Figure 2 continued.
(c) Cellular proliferation in scramble vector (SKOV3IP1 shRNA-Scramble) and CD36 shRNA transduced (SKOV3ip1 shRNA-CD36) cells was measured using a fluorescence dye that intercalates within DNA. Fluorescent readings were performed at the indicated time points and compared to a reference standard to convert sample fluorescence values into cell numbers. All data shown are means, ± s.e.m., (n=5). The experiment was repeated twice.
(d) Cellular viability in scramble vector (SKOV3IP1 shRNA-Scramble) and CD36 shRNA-1 transduced (SKOV3ip1 shRNA-CD36) cells was determined by measuring the percentage of Propidium Iodide (PI) stained cells (10 µg/mL) with flow cytometry.

Volcano plot analysis of ovarian cancer cells cultures with or without primary human adipocytes

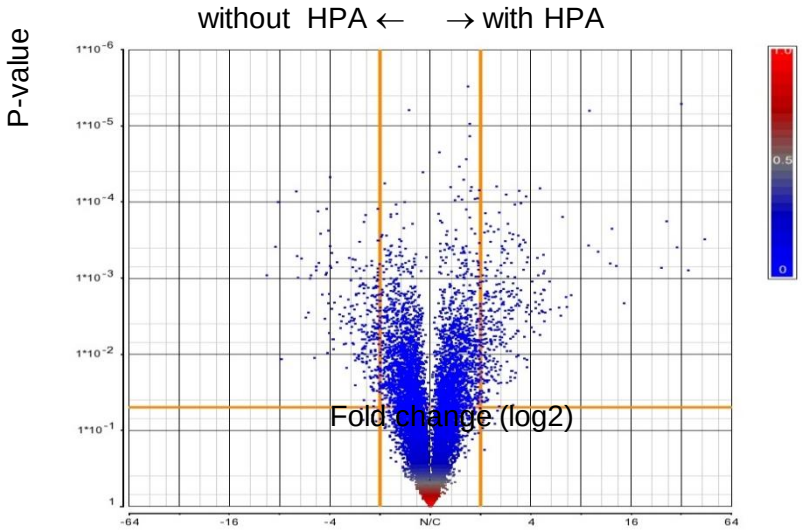

Supplementary Figure 3.
Volcano plot of Differentially Expressed Genes (DEG)s in response to adipocyte stimulation. Calculated differences of gene expression are presented by plotting the negative log 10 of P-value on the Y-axis against the log2 fold change on the X-axis. Each dot represents an individual gene..

A CD36 shRNA xenograft, immunohistochemistry

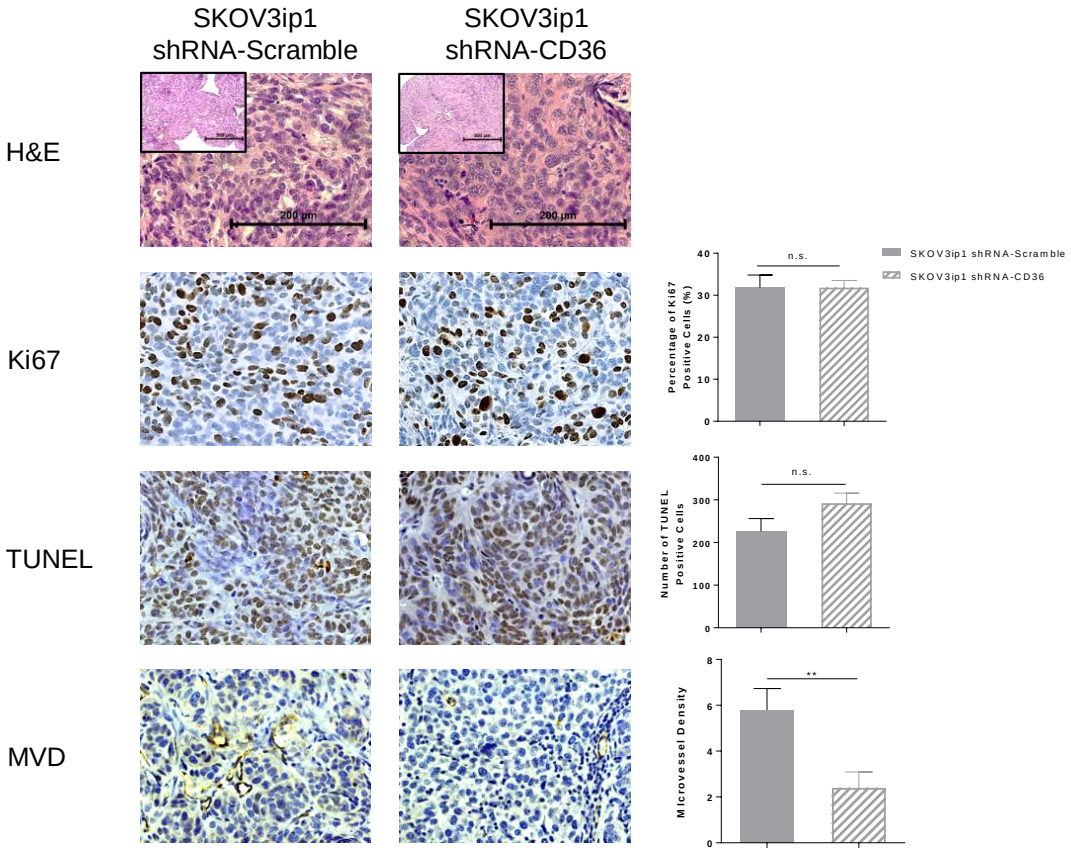

Supplementary Figure 4.
(a) Immunhistochemical analysis of mouse xenograft tumors from control (SKOV3IP1 shRNA-Scramble) and CD36 shRNA transduced (SKOV3ip1 shRNA-CD36) cells injected animals. Representative tumor areas from three different animals were stained with hematoxylin and eosin (H&E), a proliferation marker (Ki-67), an apoptosis marker (TUNEL), and an angiogenesis marker (CD31). The percentage of Ki-67 positive nuclei, the number of TUNEL positive cells per apoptotic foci and the number of microvessels (CD31) per field of were counted as described in the materials and methods. Staining quantification is on the right and representative images are on the left. Bars represent the mean ± s.e.m., **p < 0.01. n.s., not significant.

B Microvessel Density in OVCAR-8 xenograft tumors

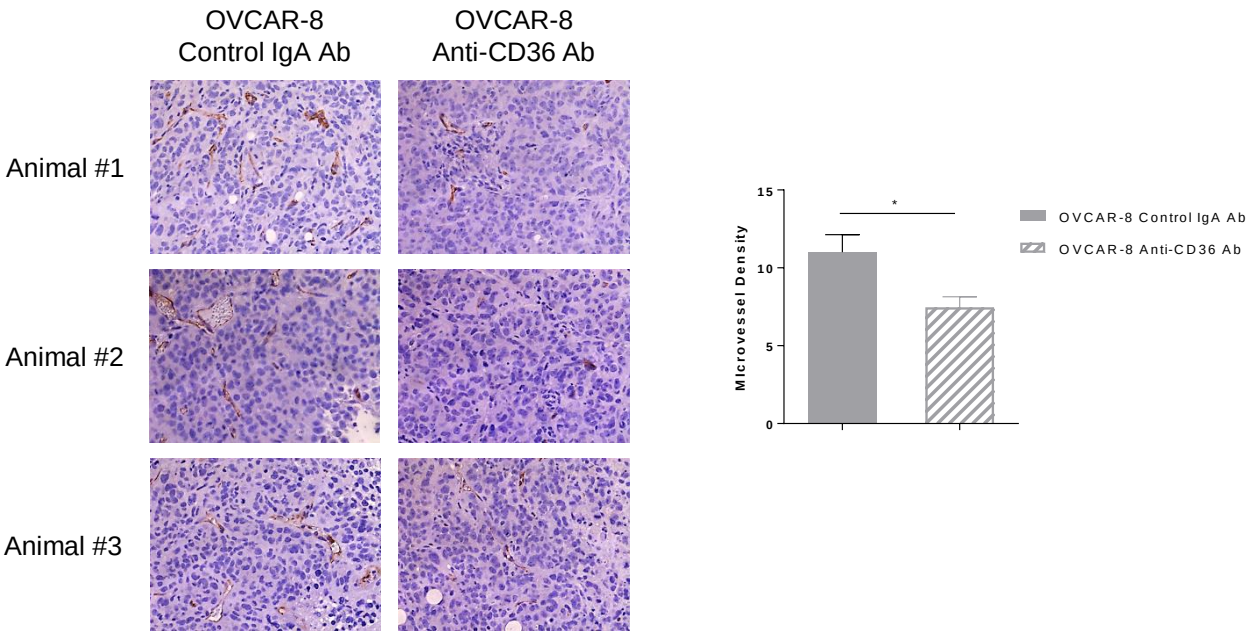

C Carbonic Anhydrase IX Staining in OVCAR-8 xenograft tumors

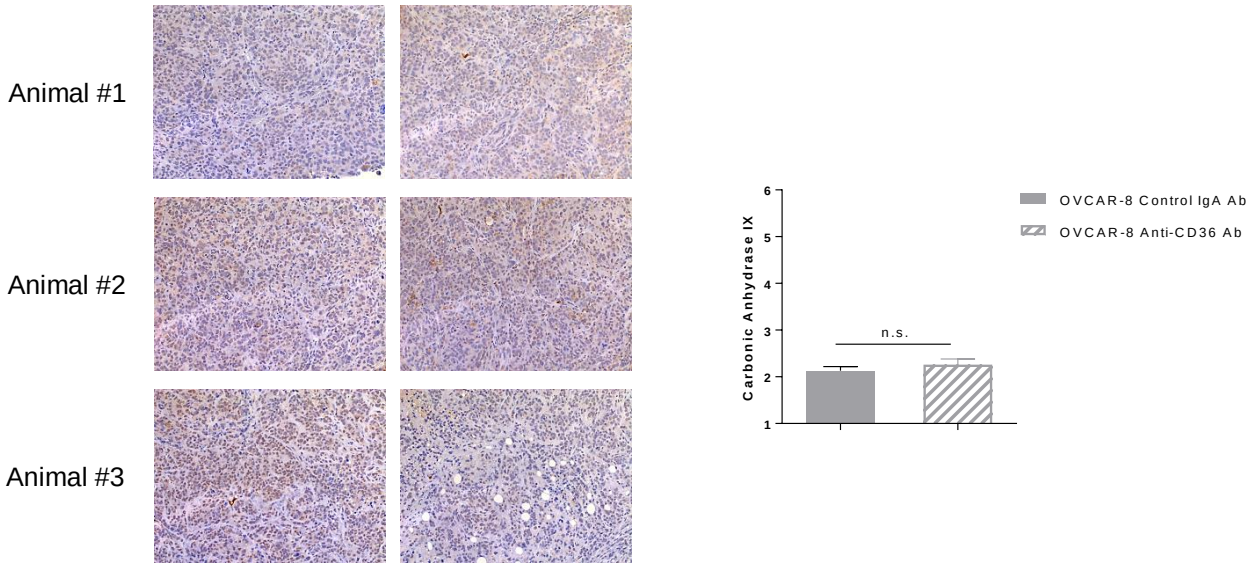

Supplementary Figure 4 continued.
Immunhistochemical analysis of mouse xenograft tumors from control (OVCAR-8 Control IgA Ab) and Anti-CD36 antibody (OVCAR-8 Anti-CD36 Ab) treated animals. Representative tumor areas from three different animals were stained with **(b)** Endothelial marker, CD31. The number of microvessels per field of were counted as described in the materials and methods **(c)** Hypoxia marker, Carbonic Anhydrase IX. Membranous staining intensity was scored as described in the materials and methods. Tumor immediately adjacent to necrotic areas were avoided. Staining quantification is on the right and representative images are on the left. Bars represent the mean ± s.e.m., *p < 0.5, n.s., not significant

D Fibronectin Content in OVCAR-8 xenograft tumors

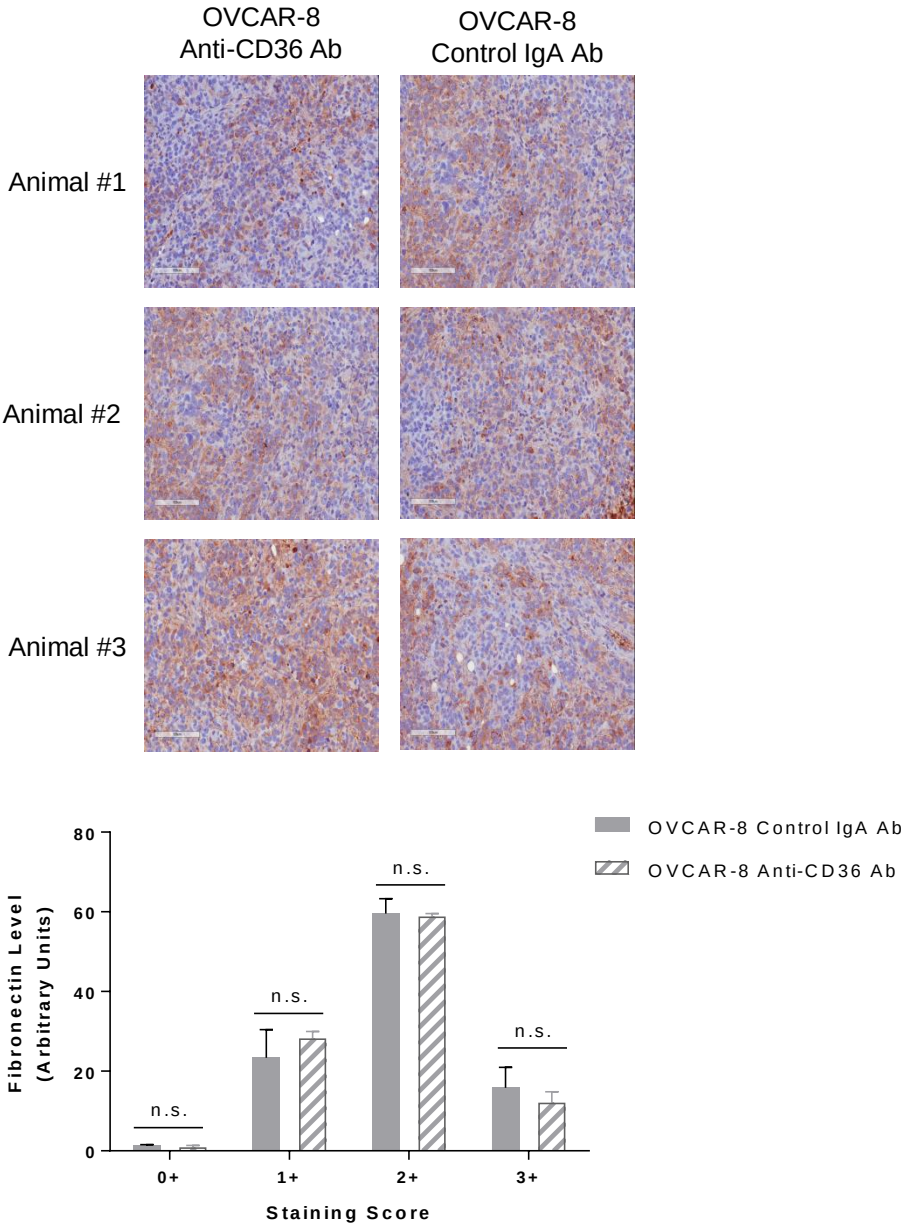

Supplementary Figure 4 continued.
Immunhistochemical analysis of mouse xenograft tumors from control (OVCAR-8 Control IgA Ab) and Anti-CD36 antibody (OVCAR-8 Anti-CD36 Ab) treated animals. Representative tumor areas from three different animals were analyzed for **(d)** fibronectin expression. Staining quantification is below and representative images are on the top. Bars represent the mean ± s.e.m., n.s., not significant

E Masson`s Trichrome Staining in OVCAR-8 xenograft tumors

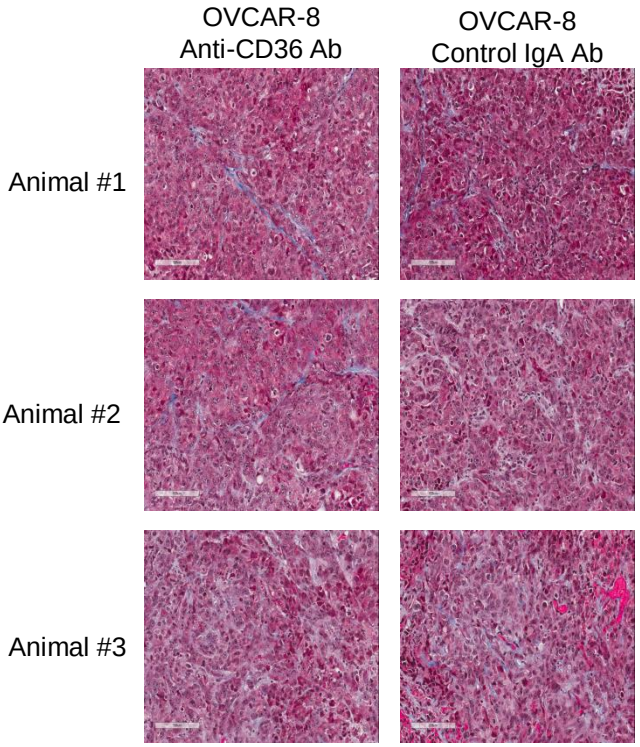

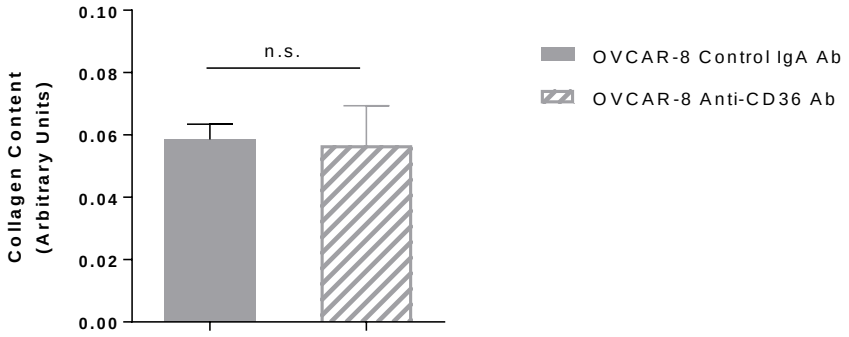

Supplementary Figure 4 continued.
Immunhistochemical analysis of mouse xenograft tumors from control (OVCAR-8 Control IgA Ab) and Anti-CD36 antibody (OVCAR-8 Anti-CD36 Ab) treated animals. Representative tumor areas from three different animals were analyzed for **(e)** collagen content. Staining quantification is below and representative images are on the top. Bars represent the mean ± s.e.m., n.s., not significant

A Laser microdissection of ovarian tumors and their metastasis

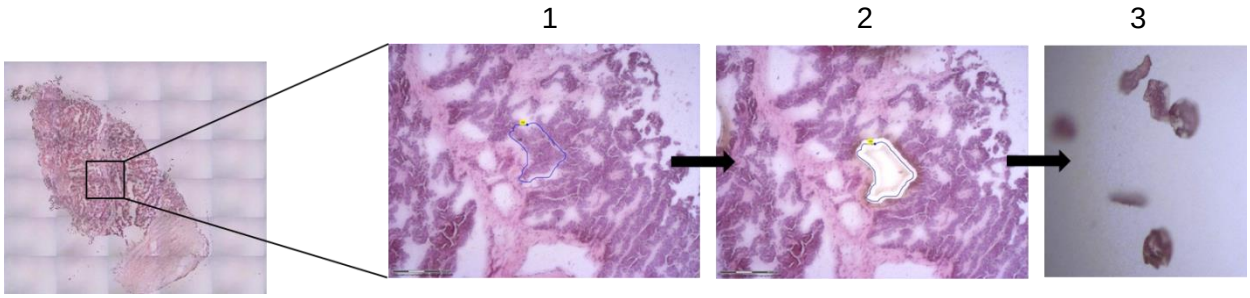

B Prognostic impact of CD36 expression

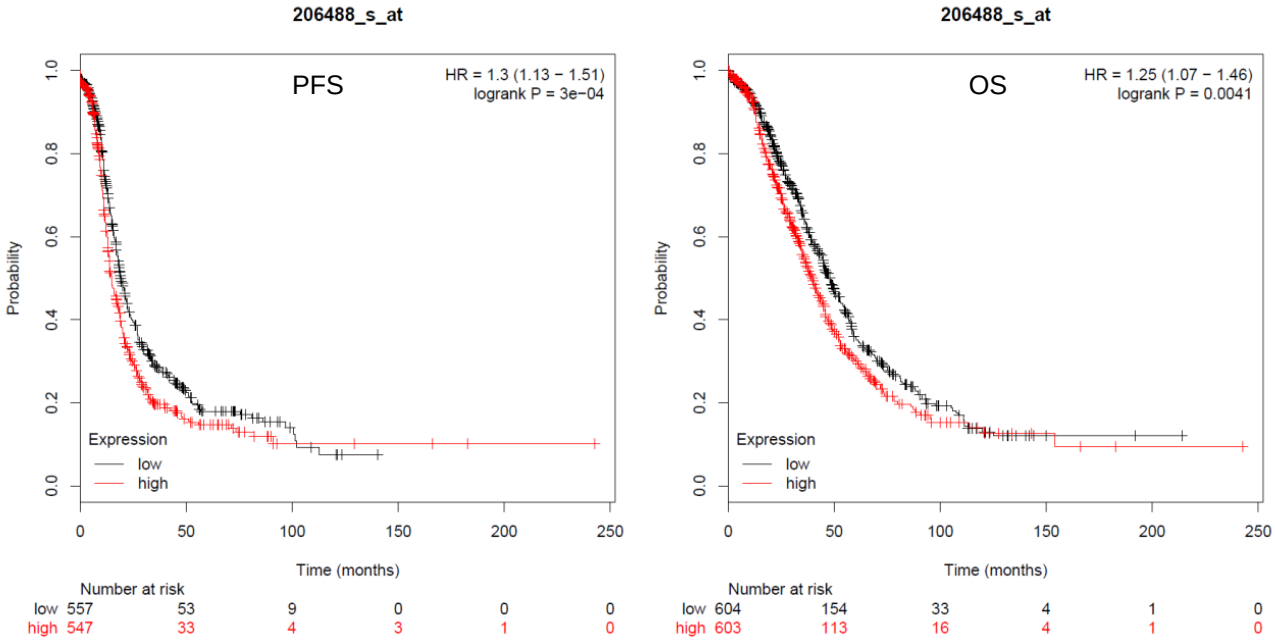

Supplementary Figure 5.
(a) Example of a laser microdissected tumor from a high-grade serous human omental metastasis sample. Left image shows a low magnification (5x) scan of the fresh-frozen tumor sample mounted on polyethylene naphthalate (PEN) membrane slide and stained with H&E stain. Right images show high (40x) magnification steps of the laser microdissection process (1) highlighting the area of interest and then cutting with a fine focused continuous laser beam, (2) re-photographed area of interest after pulsed pressure-catapulting into a microcentrifuge cap (3), and selectively harvested tumor cells in the microcentrifuge cap.
(b) Kaplan-Meier survival plots showing higher CD36 (probe 206488_s_at) expression is associated with shorter Progression Free Survival (PFS, left panel) and Overall Survival (OS, right panel) in high grade serous ovarian cancers. Plots were created in KM-plotter (http://www.kmplot.com), hazard ratio with 95% confidence intervals and log-rank P values were calculated and plotted in R using Bioconductor packages. Szasz AM et al. Oncotarget. 2016, 7:49322-49333.